α2-COP is involved in early secretory traffic in *Arabidopsis* and is required for plant growth

Fátima Gimeno-Ferrer[1]*, Noelia Pastor-Cantizano[1]*, César Bernat-Silvestre[1]*, Pilar Selvi-Martinez[1], Francisco Vera-Sirera[3], Caiji Gao[2], Miguel Angel Perez-Amador[3], Liwen Jiang[2], Fernando Aniento[1#] and María Jesús Marcote[1#]

*These authors contributed equally to the work

[1] Departamento de Bioquímica y Biología Molecular, Facultad de Farmacia, Universitat de València, E-46100 Burjassot, Spain
[2] School of Life Sciences, Centre for Cell and Developmental Biology and State Key Laboratory of Agrobiotechnology, The Chinese University of Hong Kong, Hong Kong, China.
[3] Instituto de Biología Molecular y Celular de Plantas (IBMCP), Universidad Politécnica de Valencia–Consejo Superior de Investigaciones Científicas (CSIC), E-46022 Valencia, Spain

E-mail authors: fagife@alumni.uv.es, Noelia.pastor@uv.es, Cesar.Bernat@uv.es, Pilar.selvi@uv.es, fravesi@ibmcp.upv.es, gaocaiji2@gmail.com, mpereza@ibmcp.upv.es, ljiang@cuhk.edu.hk, Fernando.aniento@uv.es, Maria.jesus.marcote@uv.es

 # To whom correspondence should be addressed
Departamento de Bioquímica y Biología Molecular
Facultad de Farmacia, Universidad de Valencia
Avenida Vicente Andrés Estellés s/n
E-46100 BURJASSOT (VALENCIA). SPAIN
Tel. + 34-963543620; Fax. +34-963544917
e-mail: mariajesus.marcote@uv.es; Fernando.aniento@uv.es

Running title: α2-COP and *Arabidopsis* early secretory pathway

Date of submission: 19th October 2016

7 Figures, 8 Supplemental Figures and 6 Supplemental Tables

Total word count: 4662

HIGHLIGHT

Arabidopsis α2-COP is required for plant growth, Golgi structure and subcellular localization of the p24 family protein p24δ5. Loss-of-function of α2-COP causes a strong up-regulation of the COPII subunit *SEC31A.*

ABSTRACT

COP(Coat Protein)I-coated vesicles mediate *intra*-Golgi transport and retrograde transport from the Golgi to the ER. COPI-coated vesicles form through the action of the small GTPase ARF1 and the COPI heptameric protein complex (coatomer), which consists of seven subunits (α-, β-, β´-, γ-, δ-, ε- and ζ-COP). In contrast to mammals and yeast, several isoforms for coatomer subunits (except γ and δ) have been identified in *Arabidopsis*. To understand the role of COPI proteins in plant biology, we have identified and characterized a loss-of-function mutant of α2-COP, an *Arabidopsis* α-COP isoform. The *α2-cop* mutant displayed defects in plant growth, including small rosettes, stems and roots and mislocalization of p24δ5, a protein of the p24 family containing a C-terminal dilysine motif involved in COPI binding. The *α2-cop* mutant also exhibited abnormal morphology of the Golgi apparatus. Global expression analysis of the *α2-cop* mutant revealed altered expression of plant cell wall-associated genes. In addition, a strong up-regulation of *SEC31A*, which encodes a subunit of the COP(Coat Protein)II coat, was observed in the *α2-cop* mutant that also occurs in a mutant of an upstream gene of COPI assembly, the ARF-GEF *GNL1*. These findings suggest that loss of *α2-COP* affects the expression of secretory pathway genes.

Key words: α1-COP, α2-COP, COP(Coat Protein)I, COP(Coat Protein)II, SEC31, Arabidopsis, p24 family protein, Golgi apparatus

INTRODUCTION

The conventional secretory pathway in plants involves the transport of newly synthesized proteins from the endoplasmic reticulum (ER) to the Golgi apparatus and to the cell surface or to the vacuole. The so-called "early secretory pathway" involves bidirectional transport between the ER and the Golgi apparatus, which is mediated by COP(Coat Protein)I and COPII vesicles (Brandizzi and Barlowe, 2013). COPII vesicles are involved in protein export from the ER, whereas COPI vesicles are involved in *intra*-Golgi transport, although their directionality is still a matter of debate, and in retrograde transport from the Golgi to the ER. Coat proteins are involved in selective capture of cargo proteins within the donor compartment, including the fusion machinery to ensure vesicle delivery, and the generation of membrane curvature to drive vesicle formation. COPI vesicles are formed at the Golgi apparatus and facilitate retrieval of ER resident proteins from the Golgi to the ER and cycling of proteins between ER and the Golgi apparatus. Many type I transmembrane proteins transported by COPI vesicles bear a C-terminal dilysine-based motif which has been proved to be recognized by the COPI coat (Jackson et al. 2012).

The key component of the COPI coat is the coatomer complex, which is essential in eukaryotes and is recruited *en bloc* onto Golgi membranes (Hara-Kuge *et al*., 1994). It is composed of seven subunits (α/β/β′/γ/δ/ε/ζ) that have been conceptually grouped into two subcomplexes, the B- (α/β/ε) and F-subcomplex (β/δ/γ/ζ). The B-subcomplex has been proposed to function as the outer layer and the F-subcomplex as the inner layer of the vesicle coat (Jaskson, 2014). However, recent structural studies revealed that the subunits are highly connected to each other, indicating that COPI structure does not fit with the adaptor F-subcomplex and cage B-subcomplex structure described for other coats (Dodonova *et al*., 2015). Following recruitment by the small GTPase ARF1, in its GTP-bound conformation, and cargo, COPI polymerizes on the membrane surface in such a way that COPI coat assembly depends on both membrane and cargo binding. Several studies indicate that the β′-COP and α–COP subunits are involved in cargo binding (i.e. proteins with a dilysine motif) through their N-terminal WD repeat domains. It has also been reported that the γ subunit interacts with ARF1 and that ζ-COP is required for the stability of γ-COP (Jackson, 2014).

Genes encoding the components of the COPI machinery have been identified in plants (Robinson *et al*., 2007; Gao *et al*., 2014; Ahn *et al*., 2015; Woo *et al*., 2015). In *Arabidopsis*, several isoforms of all the coatomer subunits, except for γ-COP and δ-COP subunits, have been identified. This is in contrast to mammals, where only γ-COP and ζ-COP subunits have more than one isoform, and yeast, that contains only one isoform for every subunit. Interestingly, electron tomography studies in *Arabidopsis* have identified two structurally distinct types of COPI vesicles (Donohoe *et al*., 2007; Gao *et al*., 2014). These different subpopulations of COPI vesicles might be formed by different coatomer isoforms. Therefore, it is of great interest to know whether these different COPI subunits isoforms have specific biological functions in plants by means of their functional characterization. Recently, the subcellular localization, protein interaction and physiological functions of β′-, γ-, and δ-COP subunits were investigated in *Nicotiana benthamiana* and tobacco BY-2 cells. It was shown that the COPI complex is involved in Golgi maintenance and cell-plate formation, and that programmed cell death is induced after prolonged COPI depletion (Ahn *et al*., 2015). In *Arabidopsis*, knock-down of ε-COP subunit isoforms has been reported to cause severe morphological changes in the Golgi apparatus and mislocalization of endomembrane proteins (EMPs) containing the KXD/E COPI interaction motif (Woo *et al*., 2015). Here, we have used a loss-of-function approach to characterize the *Arabidopsis* α2-COP isoform. Two α-COP isoforms, α1-COP (At1g62020) and α2-COP (At2g21390), have been identified in *Arabidopsis* and both isoforms contain an N-terminal WD40 domain that may allow them to recognize C-terminal dilysine-based motifs of COPI cargo proteins (Eugster *et al*., 2004; Jackson *et al*., 2012). We found that a loss of function mutant of *α2-COP* showed defects in growth. In addition, in the *α2-cop* mutant, the subcellular localization of p24δ5, a protein with a dilysine motif that has been shown to cycle between ER and the Golgi, as well as the morphology of the Golgi apparatus was altered. A transcriptomic analysis of the *α2-cop* mutant showed up-regulation of plant cell wall and endomembrane system genes, like the COPII component *SEC31A* gene, indicating that *α2-cop* loss of function affects the expression of secretory pathway genes.

MATERIALS AND METHODS

Plant material

Arabidopsis thaliana ecotype Col-0 was used (wild type). The loss-of-function mutants *α1-cop-1* (SALK_078465), *α2-cop-1* (SALK_103968) and *α2-cop-2* (SALK_ 1229034) and *gnl1* (SALK_091078C) were from the Salk Institute Genomic Analysis Laboratory (http://signal.salk.edu/cgi-bin/tdnaexpress). *α2-cop-3* (GABI_894A06) was from GABI-Kat (Kleinboelting *et al*., 2012). All the mutants were obtained from the Nottingham Arabidopsis Stock Centre. *Arabidopsis thaliana* plants were grown in growth chambers as previously described (Ortiz-Masia *et al*., 2007). Lines (Col-0 background) containing a T-DNA insertion described above were characterized by PCR. The primers used are included in Supplemental Table S6.

Recombinant plasmid production, plant transformation and transformant selection

The coding sequence of *α2-COP* with one HA tag before the stop codon was synthesized commercially *de novo* (Geneart AG) based on the sequence of *α2-COP* (At2g21390). The coding sequence of *α2-COP-HA* was cloned into the pCHF3 vector (carrying the CaMV 35S promoter) (Ortiz-Masia et al., 2007) through SmaI/SalI. To complement growth defects, *α2-cop-3* plants were transformed with the *α2-COP-HA* construction via Agrobacterium by floral deep method according to standard procedures (Clough and Bent 1998). To estimate the number of T-DNA insertions in the transgenic plants, 40 seeds of each T1 line were plated on 1/2 xMS basal salts, 1% sucrose, 0.6% agar with 50 mg/l kanamycin. Only lines where the proportion of kanamycin resistant to sensitive plants in their progeny fitted to a 3:1 ratio were considered. Homozygous *α2-COP-HA* T2 lines were identified by the same method.

For confocal studies, *α2-cop-3* and wild type plants were transformed with a ST-YFP construct (kindly provided by Dr. DG Robinson, Heidelberg, Germany) and a RFP-p24δ5 construct as described above. The RFP-p24δ5 construct was obtained by subcloning the RFP-p24δ5 coding sequence (Langhans *et al*., 2008) in the pCHF3 vector through KpnI/BamHI. The transformants were selected with antibiotic as above.

We obtained three independent ST-YFP- and RFP-p24δ5-*α2-cop-3* lines that show the same confocal phenotypes, over subsequent generations.

RT-PCR

Total RNA was extracted from seedlings using a Qiagen RNeasy plant mini kit and 3 µg of the RNA solution were reverse-transcribed using the maxima first-strand cDNA synthesis kit for quantitative RT-PCR (Fermentas) according to the manufacturer's instructions. Semi-quantitative PCRs (sqPCRs) were performed on 3-µL cDNA template using the kit PCR Master (Roche). The sequences of the primers used for PCR amplifications are included in Supplemental Table S6.

Quantitative PCR (qPCR) was performed using a StepOne Plus of Applied Biosystems with the SYBR Premix Ex Taq TM (Tli RNaseH Plus) (Takara) according to the manufacturer's protocol. Each reaction was performed in triplicate with 100 ng of the first-strand cDNA and 0.3 µM of primers for all the genes and 0.9µM for *SEC31A* in a total volume of 20 µl. Data are the mean of two biological samples. The specificity of the PCR amplification was confirmed with a heat dissociation curve (from 60°C to 95°C). Relative mRNA abundance was calculated using the comparative Ct method according to Pfaffl (2004). Primers used for quantitative PCR (qPCR) are listed in Supplemental Table S6.

Preparation of protein extracts and Western-blotting

7-day-old seedlings were ground in liquid nitrogen and homogenised in lysis buffer, 50 mM TRIS-HCl pH 7.5, 150 mM NaCl, 0.5 mM DTT, 0.5% Triton X-100, and a cocktail of protease inhibitors (1:250 dilution, Sigma #P9599) for 30 min at 4 °C. Samples were centrifuged twice at 12,000g for 20 min at 4°C and supernatants were considered as protein extracts. Protein quantitation was performed with Bradford assay (Bio-Rad Laboratories GmbH, Munich, Germany). Protein samples were separated by electrophoresis on a 8% SDS-polyacrylamide gel and transferred to nitrocellulose membranes (Schleicher & Schuell). Before blotting, membranes were stained with Ponceau-S solution (Sigma) to show loading of the protein samples. Membranes were

probed with the primary antibody anti-HA High Affinity (Roche) (1:500), Anti-human GAPC (Santa Cruz) (1:1000) or anti-α-COP (1:2000) (Gerich *et al.*, 1995); and developed by ECL (Enhanced Chemiluminescence; GE Healthcare) as previously described (Montesinos *et al.*, 2013). Western blots were analyzed using the ChemiDoc XRS+ imaging system (Bio-Rad, http://www.bio-rad.com/).

Microarrays

4-day-old seedlings (*α2-cop-3* and wild-type) grown in 1/2 MS plates were used. Total RNAs from 4 pools of seedlings were extracted using the RNeasy plant mini kit (Qiagen), and RNA integrity was tested by 2100 Bioanalyzer (Agilent). The four replicas of WT were pooled together to generate a unique reference sample, that was tested against each of the individual *α2-cop-3* samples to generate 4 biological independent assays, in two-color assay with dye-swap. RNA labeling and microarray details were as described in Vera-Sirera *et al*. (2015). Half microgram of RNA per sample was amplified and labelled with the Agilent Low Input Quick Amp Labelling Kit. Agilent Arabidopsis (V4) Gene Expression 4344K Microarray were used. Hybridization and slide washing were carried out with the Gene Expression Hybridization Kit and Gene Expression Wash Buffers. Slides were scanned in an Agilent G2565AA microarray scanner at 5 µm resolution in dual scan for high dynamic. Image files were analyzed with the Feature Extraction software 9.5.1. Raw microarray data (accession number GSE81049) were deposited in the Gene Expression Omnibus (GEO). Inter-array analysis were performed with the GeneSpring 11.5 software. Only features for which the 'r or/and gIsWellAboveBG' parameter was 1 at least in three out of four replicas were selected. T-test analysis was carried out with Benjamin-Hochberg metrics to identify significantly expressed genes with p-value below 0.05 after correction for multiple-testing, and expression ratio was above or below two-fold difference (Log_2 ±1). Features were converted into genes based in a BLAST analysis extracted from ftp://ftp.arabidopsis.org/Microarrays/Agilent/; oligo probes that that did not correspond to any gene or to more than one gene were removed for further analysis. Gene Ontology (GO) analysis of the Biological Process level was carried out with the

agriGO (http://bioinfo.cau.edu.cn/agriGO/; Du *et al*., 2010). Only GO terms with corrected p-value ≤0.05 were selected.

Transmission electron microscopy

For electron microscopy, seedlings were grown on MS medium containing 1 % agar, and the seedlings were harvested after 4 days. Chemical fixation of cotyledons was performed according to Osterrieder et al. (2010). Ultrathin (70 nm) sections were cut on a Microtome Leica UC6, stained with uranyl acetate and lead citrate and observed with a JEM-1010 (JEOL) transmission electron microscope. High-pressure freezing was performed as described previously (Tse *et al*., 2004; Gao *et al*.., 2012) and samples were analysed in a Hitachi H-7650 transmission electron microscope.

Confocal microscopy

Imaging was performed using an Olympus FV1000 confocal microscope (http://www.olympus.com/) with a 60× water lens. Fluorescence signals for YFP (514 nm/529–550 nm) and RFP (543 nm/593–636 nm) were detected. Sequential scanning was used to avoid any interference between fluorescence channels. Post-acquisition image processing was performed using the fv10-asw 3.1 Viewer and coreldrawx4 (14.0.0.567) or ImageJ (version 1.45 m) (Abramoff *et al*., 2004).

RESULTS

α2-cop mutants display a dwarf phenotype

To investigate the function of the two isoforms of the α-COP subunit in *Arabidopsis*, T-DNA insertion mutants were identified and analyzed. A mutant of α1-COP, *α1-cop-1*, that had the insertion in the third coding exon, was identified in the Salk collection, corresponding to stock number SALK_078465 (Figure 1A). Although truncated transcripts were detected (Supplemental Figure S1), RT-PCR analysis confirmed that this mutant lacked the full length α1-COP transcript (Figure 1B). As it is shown in Figure 1C, *α1-cop-1* mutation did not compromise plant growth under standard growth conditions

Three mutants of α2-COP, *α2-cop-1* (SALK_103968), *α2-cop-2* (SALK_ 1229034) and *α2-cop-3* (GABI_894A06) that had the insertion in different gene positions (Figure 2A) were characterized. Homozygous plants were selected and RT-PCR analysis confirmed that *α2-cop-1*, *α2-cop-2* and *α2-cop-3* mutants lacked the full length α2-COP transcript (Figure 2B). As it happened in the *α1-cop-1* mutant, truncated transcripts were detected in the *α2-cop* mutants (Supplemental Figure S1). In contrast to the normal growth of *α1-cop-1*, all *α2-cop* mutants exhibited dwarf phenotypes, with reduced rosette and leaf size and shorter stems and roots although they were all fertile (Figure 2C and Supplemental Figure S2).

In this work, we focused on the characterization of the *α2-cop-3* mutant for further analysis of *α2-COP* loss of function (Figure 2). To confirm that the developmental defects in *α2-cop-3* were indeed caused by the loss of α2-COP function, we transformed it with an α2-COP cDNA containing an HA tag. As it is shown in Figure 2D, the expression of α2-COP-HA in the *α2-cop-3* mutant fully rescued its developmental defects. These results indicate that α2-COP may be required for normal plant growth and development.

Next, the expression levels of total *α-COP* in *α1-cop* and *α2-cop* mutants were analyzed compared to wild type, to investigate whether the dwarf phenotype of *α2-cop* was due to lower expression levels of *α-COP*. To this end, the expression levels of total

α-COP (including isoforms α1 and α2) were analyzed by RT-PCR using a pair of primers (α125 and α123) common to *α1-COP* and *α2-COP* genes (Figures 1 and 2) that can therefore amplify the cDNA of both genes in wild type plants. However, these primers can only amplify the *α2-COP* cDNA fragment (and not the *α1-COP* cDNA fragment) in the *α1-COP* mutant due to the presence of the T-DNA insertion in the mutant. Similarly, these primers can only amplify the *α1-COP* cDNA fragment (and not the *α2-COP* cDNA fragment) in the *α2-cop* mutant. As it is shown in Figure 3A-C, mRNA levels of α-COP were lower in *α2-cop* than in *α1-cop* mutant, which correlates with the growth defects in *α2-cop-3*. On the other hand, the mRNA levels of *α1-COP* and *α2-COP* in *α2-cop-3* and *α1-cop-1-1* mutants, respectively, were similar to those in the wild type (Supplemental Figure S3), indicating that there is no expression compensation between the two *α-COP* genes in the mutants. Therefore, these results suggest that the two α-COP isoforms are differently expressed and it is the *α2-COP* isoform the one that contributes more to the total of α-COP. Then, the protein levels of α-COP (α1 plus α2 isoforms) were analyzed by Western blot using an antibody against the 10 first aminoacids of cow α-COP (Gerich *et al*., 1995) that has been previously described to recognize *Arabidopsis* α-COP (Contreras *et al*., 2004a). As cow α-COP and both *Arabidopsis* α-COP isoforms share the first 9 aminoacids, this antibody should recognize both isoforms. As it is shown in Figure 3D, the antibody recognized a band of aproximately 130 kDa corresponding to the molecular weight of α-COP. Using this antibody, we found that the *α2-cop-3* mutant has also lower α-COP protein levels than wild type and the *α1-cop* mutant (Figure 3D). No specific bands from translation of truncated transcripts were detected in the mutants (Supplemental Figure S1).

The loss of function of *α2-COP* affects p24δ5 trafficking and the integrity of the Golgi apparatus

As the *α2-cop* mutant has defects in growth, we aimed to study if retrograde transport in the early secretory pathway was impaired in this mutant. COPI vesicles have been involved in the traffic of some transmembrane proteins that constitutively cycle between the ER and the Golgi by using the COPII and the COPI systems, such as members of

the p24 family. p24 proteins constitute a family of type-I transmembrane proteins of approximately 24 kDa present on the membranes of the early secretory pathway (Pastor-Cantizano *et al*., 2016). We have previously shown that the C-terminal cytosolic tail of *Arabidopsis* p24δ subfamily proteins has the ability to interact with ARF1 and coatomer subunits (through a dilysine motif) and with COPII subunits (through a diaromatic motif) (Contreras *et al*., 2004a,b). Using a fluorescence-tagged version of one member of the p24 family (RFP-p24δ5), we have also shown that p24δ5 localizes to the ER at steady state as a consequence of highly efficient COPI-based recycling from the Golgi apparatus and that the dilysine motif is necessary and sufficient for ER localization (Contreras *et al*., 2004a,b; Langhans *et al*., 2008; Montesinos *et al*., 2012). More recently, we have found that p24δ5 interacts with ARF1 and COPI subunits at acidic pH, consistent with this interaction taking place at the Golgi apparatus (Montesinos *et al*., 2014). Therefore, we used p24δ5 as a model protein to study COPI-dependent retrograde Golgi-to-ER trafficking in the *α2-cop* mutant. In wild type plants, RFP-p24δ5 mostly localized to the ER network (Figure 4), as described previously (Sancho-Andrés et *al*, 2016). In contrast, RFP-p24δ5 localized only partially to the ER and was mostly found in punctate structures, which often appeared in clusters, in the *α2-cop-3* mutant (Figure 4). Next, we also checked the distribution of sialyl transferase-YFP (ST-YFP), a specific membrane marker for the plant Golgi (Boevink *et al*., 1998), in the *α2-cop-3* mutant. As it is shown in Figure 5, ST-YFP showed the typical punctate pattern characteristic of normal Golgi stacks in wild type plants. However, in the *α2-cop-3* mutant ST-YFP localized partially to the ER network and to clusters of punctate structures (Figure 5).

To gain insight into the defects observed in the *α2-cop*-3 mutant at the ultrastructural level, we performed transmission electron microscopic (TEM) analysis of ultrathin sections using seedlings processed either by chemical fixation (Figure 6A) or high-pressure freezing/freeze substitution (Figure 6B). As shown in this Figure, the *α2-cop* mutant showed a clear alteration in the Golgi apparatus, which in most cases had a reduced number of cisternae per Golgi stack. In addition, the *α2-cop* mutant also contained many abnormal vesicle clusters around the Golgi remnants.

Transcriptomic analysis of *α2-cop* mutant

Comparative gene expression analysis were performed to gain insight of the molecular phenotype of the *α2-cop-3* mutant. Global profiling analysis was carried out from 4-day-old seedlings, when the mutant growth phenotype starts to be visible, to detect early changes in expression. A median $\log_2$ ratio of 1 (2-fold difference in expression) of the four biological replicates was used as a cut-off criteria to compare the mutant with wild type plants. We identified 534 differentially expressed genes in the *α2-cop-3* mutant, distributed in 353 induced (ratio > 1) and 181 repressed (ratio < 1) (Supplemental Tables S1 and S2, respectively). Confirmation of microarray data was carried by RT-PCR in the *α2-cop-3* (Figure 7A) as well as in the *α2-cop-1* and *α2-cop-2* mutants (Supplemental Fig. S4). Gene Ontology analysis was performed by agriGO (Du *et al*., 2010) and GO terms that were overrepresented among up-regulated genes (Supplemental Figures S5-S7 and Supplemental Table S3) and down-regulated genes (Supplemental Figure S8 and Supplemental Table S4) were selected. Interestingly, the most significantly overrepresented GO Cellular Component terms among the up-regulated genes were "plant-type cell wall" and "endomembrane system" (Supplemental Tables S3 and S5). On the other hand, GO terms significantly overrepresented in Biological Process were "lipid transport" and "cell wall modification" and "oligopeptide transport activity" related to the GO of Molecular Functions (Supplemental Table S3).

Interestingly, one of the genes highly upregulated was *SEC31A*, that encodes one subunit of the COPII coat. The *Arabidopsis* genome encodes two SEC31 isoforms, SEC31A (At1g18830) and SEC31B (At3g63460). Confirming the microarray data, RT-PCR analysis indicated that the expression of *SEC31A* in the *α2-cop-3* mutant is more than ten times higher than in wild type (Fig. 7B). *SEC31A* expression was also slightly induced (two fold) in the *α1-cop-1* mutant. On the other hand, *SEC31B* expression was not up-regulated either in the *α2-cop-3* or in the *α1-cop-1* mutant. This strong up regulation of *SEC31A* in the *α2-cop-3* mutant is consistent with the COPII machinery being transcriptionally regulated by the alteration in the COPI traffic. However, this up-regulation of SEC31A seems to be specific for this COPII subunit, as the expression other COPII subunit genes did not change in the *α2-cop3* mutant (Figure 7C and Supplemental Tables S1 and S2). Finally, we also analysed the expression of *SEC31A* in

gnl1 (SALK_091078C), a loss-of-function mutant of the ADP-ribosylation factor guanine nucleotide-exchange factor (ARF-GEF) GNL1 that regulates COPI formation (Richter *et al*., 2007; Teh and Moore, 2007; Nakano *et al*., 2009; Du *et al*., 2013). Figure 7D shows that the pattern of activation/repression of some of the genes that were used to confirm the microarray data of the *α2-cop3* mutant, was similar in the *gnl1* mutant, including increased expression of SEC31A, suggesting a correlation between the alteration in COPI function and changes in the expression of the COPII subunit *SEC31A*.

DISCUSSION

In mammals and yeast there is only one isoform of the COPI subunit α-COP. In contrast, two α-COP isoforms, α1- and α2-COP, have been identified in *Arabidopsis*. In this work, we have shown that a knockout T-DNA mutant of *α1-COP* resembled wild type plants under standard growth conditions. However, all *α2-COP* T-DNA mutants characterized had defects in root, stem and leaf growth. They were all fertile but short and bushy. The two α-COP isoforms contain at their N-terminal the WD40 domain, that it is required for KKXX-dependent trafficking. It cannot be ruled out that a truncated α-COP protein might be synthesized in the mutants that could account for the difference in the phenotypes between *α1-COP* and *α2-COP* mutants, although no truncated proteins were detected with an N-terminal antibody by Western blot. On the other hand, as both isoforms showed 93% of amino acid sequence identity, the absence of growth defects in the *α1-cop* mutant might be explained by the relative expression levels of both α-COP isoforms. Nevertheless, it cannot be discarded that α2-COP may have specific functions that cannot be performed by α1-COP. Further studies will be required to clarify the differences between the functions of α1-COP and α2-COP. In this study we focused on the characterization of the *α2-cop-3* mutant. As the expression of α2-COP-HA in the *α2-cop-3* mutant fully rescued its developmental defects, the results presented here indicate that α2-COP has a role in plant growth.

COPI vesicles are involved in the retrieval of ER-resident proteins from the Golgi apparatus to the ER and also in the traffic of other transmembrane proteins found in the early secretory pathway that are continuously cycling between ER and Golgi, as it is the case of p24 family proteins. *Arabidopsis* p24δ proteins contain in their cytosolic C-terminus both a dilysine motif in the -3,-4 position, involved in COPI interaction through α-COP and β´-COP subunits (Jackson *et al.*, 2012; Eugster, 2004) and a diaromatic motif in the -7,-8 position involved in COPII binding (Contreras *et al*., 2004b). At steady state, p24δ5 mainly localizes to the ER as a consequence of its highly efficient COPI-based recycling from the Golgi apparatus (Langhans *et al*., 2008; Montesinos *et al*., 2012; 2013; 2014; Sancho-Andrés et al. 2016). Here, we have found that loss of *α2-COP* causes obvious defects in trafficking of RFP-p24δ5, which mostly localized to clusters of punctate structures and was only partially found at the ER network. This probably reflects the inability of p24δ5 to enter standard COPI vesicles for its Golgi to ER retrograde transport. In addition, the localization of the Golgi marker ST-YFP was also altered, which might be the result of fragmentation of the Golgi apparatus, consistent with recent reports showing that silencing of ε-COP and δ-COP in *Arabidopsis* and β′-COP in *N. benthamiana* results in disruption of Golgi structure (Ahn *et al*., 2015; Woo *et al*., 2015). Indeed, the ultrastructural studies of the *α2-cop-3* mutant revealed severe morphological changes in the Golgi apparatus. These results confirm the role of COPI in mantaining normal cellular function and organelle morphology in the plant early secretory pathway, as previously described in mammals and yeast (Guo *et al*., 1994; Gaynor and Emr, 1997; Styers *et al*., 2008).

Results from the microarray revealed up-regulation of plant cell wall and endomembrane system genes. As most of these genes encoded proteins that follow or regulate the secretory pathway, this change of gene expression could be a mechanism to compensate failures in the secretory pathway of the mutant due to the absence of α2-COP. Interestingly, one of the up regulated genes in the *α2-cop-3* mutant was the *SEC31A* gene, that encodes one of the two COPII SEC31 isoforms of *Arabidopsis*. No changes in COPII subunits other than SEC31A have been detected. SEC31A shows 61% amino acid sequence identity with SEC31B and according to public microarray data (Zimmermann *et al*., 2004), they are differently expressed in *Arabidopsis* tissues,

being *SEC31B* expression about ten times higher than that of *SEC31A*. It has been reported that SEC31B is not able to complement the secretion defect of the *sec31-1* mutant in yeast (De Craene *et al*., 2014). In that study, SEC31A was not tested and the authors concluded that SEC31A could be the one that complements the secretion defect of the *sec31-1* mutant. In mammals, two SEC31 isoforms have also been identified but their specific roles have not been defined yet. On the other hand, there is evidence that SEC31 interacts directly with SAR1 (the small GTPase that controls COPII vesicle biogenesis) to promote SEC23 GAP activity (Bi *et al*., 2007). It has been proposed that differences in affinity for SEC31 between mammalian paralogs of SAR1 together with changes in the stimulated rate of GTP-hydrolysis may cooperate with the intrinsic flexibility of the outer cage in determining COPII vesicle size during the dynamic process of assembly and disassembly of the coat on a growing bud (Zanetti *et al*., 2011). There is increasing evidence that indicates that specific expression patterns in COPII subunit isoforms in *Arabidopsis* may reflect functional diversity (Chung et *al*, 2016). Since the expression of SEC31A was highly increased in the *α2-cop* mutant, SEC31A could compete with SEC31B for SAR1 binding resulting in changes in the process of assembly and disassembly of the coat that could adapt ER export machinery under these conditions. The induction of SEC31A might enable efficient packaging of specific cargo proteins into anterograde vesicles or simply increase the overall capacity of anterograde transport to compensate the effects of the inhibition of retrogade transport in the *α2-cop* mutant. Interestingly, *SEC31A* is also up-regulated in the unfolded protein response (UPR), mediated by the inositol requiring enzyme-1 (IRE1), a response that is known to result in a specific remodeling of the secretory pathway (Nagashima *et al*., 2011; Song et al. 2015). Finally, we also found that *SEC31A* is also strongly up-regulated in *gnl1*, a mutant of the ARF-GEF GNL1 involved in COPI assembly. These data suggests that the increase in *SEC31A* expression might be part of a general response to alterations of the secretory pathway.

413 **SUPPLEMENTARY DATA**

414

415 **Supplemental Figure S1.** sqRT-PCR and Western blot analysis of *α1-cop* and *α2-cop*
416 mutans to detect truncated transcripts and proteins, respectively**.**

417 **Supplemental Figure S2.** *α2-cop* mutants show the same growth phenotype.

418 **Supplemental Figure S3.** RT-qPCR analysis of *α1-COP* and *α2-COP* expression in
419 *α2-cop-3* and *α1-cop-1* mutants, respectively.

420 **Supplemental Figure S4.** Confirmation of the *α2-cop-3* microarray data in the other
421 two *α2-cop* mutans

422 **Supplemental Figure S5.** Hierarchical view of Gene Ontology (GO) categories
423 significantly over-represented among the up-regulated genes in the *α2-cop-3* mutant.
424 Biological Process terms.

425 **Supplemental Figure S6.** Hierarchical view of Gene Ontology (GO) categories
426 significantly over-represented among the up-regulated genes in the *α2-cop-3* mutant.
427 Cellular component terms.

428 **Supplemental Figure S7.** Hierarchical view of Gene Ontology (GO) categories
429 significantly over-represented among the up-regulated genes in the *α2-cop-3* mutant.
430 Molecular function.

431 **Supplemental Figure S8.** Hierarchical view of Gene Ontology (GO) categories
432 significantly over-represented among the down-regulated genes in the *α2-cop-3* mutant.

433 **Supplemental Table S1.** List of upregulated genes in the *α2-cop-3* mutant.

434 **Supplemental Table S2.** List of downregulated genes in the *α2-cop-3* mutant.

435 **Supplemental Table S3.** Non-redundant Gene Ontology (GO) categories significantly
436 overrepresented among up-regulated genes in the *α2-cop-3* mutant.

437 **Supplemental Table S4.** Non-redundant Gene Ontology (GO) Biological Process
438 categories significantly overrepresented among the down-regulated genes in the *α2-cop-*
439 *3* mutant.

Supplemental Table S5. Plant cell wall and endomembrane up regulated genes in the *α2-cop-3* mutant.

Supplemental Table S6. Primers used in this study.

ACKNOWLEDGEMENTS

Antibody against α-COP was kindly provided by Prof. F. Wieland. This work was supported by the Ministerio de Economía y Competitividad (grant no. BFU2012–33883 to F.A. and M.J.M; grants no BIO2011-26302 and BIO2014-55946-P to M.P.), the Generalitat Valenciana (grant nos. ISIC/2013/004 and GVACOMP2014–202 to F.A. and M.J.M.) and the Research Grants Council (grant no AoE/M-05/12 to L.J.). N.P. and C.B. were recipients of a fellowship from Ministerio de Educacion (FPU program). We thank the Salk Institute Genomic Analysis Laboratory for providing the sequence-indexed *Arabidopsis* T-DNA insertion mutants and the microscopy and genomics section of SCSIE (University of Valencia).

REFERENCES

Abramoff MD, Magelhaes PJ, Ram SJ. 2004. Image Processing with ImageJ. Biophotonics International **11**, 36-42.

Ahn HK, Kang YW, Lim HM, Hwang I, Pai HS. 2015. Physiological Functions of the COPI Complex in Higher Plants. Molecules and Cells **38,** 866-875.

Bi X, Mancias JD, Goldberg J. 2007. Insights into COPII coat nucleation from the structure of Sec23.Sar1 complexed with the active fragment of Sec31. Developmental Cell **13**, 635-645.

Boevink P, Oparka K, Santa Cruz S, Martin B, Betteridge A, Hawes C. 1998. Stacks on tracks: the plant Golgi apparatus traffics on an actin/ER network. Plant Journal **15**, 441-447.

Brandizzi F, Barlowe C. 2013. Organization of the ER-Golgi interface for membrane traffic control. Nature Reviews Molecular Cell Biology **14,** 382-392.

Chung KP, Zeng Y, Jiang L. 2016. COPII Paralogs in Plants: Functional Redundancy or Diversity? Trends in Plant Science doi: 10.1016/j.tplants.2016.05.010.

Clough SJ, Bent AF. 1998. Floral dip: a simplified method for Agrobacterium-mediated transformation of *Arabidopsis thaliana*. Plant Journal **16,** 735-743.

Contreras I, Ortiz-Zapater E, Aniento F. 2004a. Sorting signals in the cytosolic tail of membrane proteins involved in the interaction with plant ARF1 and coatomer. Plant Journal **38,** 685-698.

Contreras I, Yang Y, Robinson DG, Aniento F. 2004b. Sorting signals in the cytosolic tail of plant p24 proteins involved in the interaction with the COPII coat. Plant Cell Physiology **45,** 1779-1786.

De Craene JO, Courte F, Rinaldi B, Fitterer C, Herranz MC, Schmitt-Keichinger C, Ritzenthaler C, Friant S. 2014. Study of the plant COPII vesicle coat subunits by functional complementation of yeast *Saccharomyces cerevisiae* mutants. PLoS One **9,** e90072.

Dodonova SO, Diestelkoetter-Bachert P, von Appen A, Hagen WJ, Beck R, Beck M, Wieland F, Briggs JA. 2015. VESICULAR TRANSPORT. A structure of the COPI coat and the role of coat proteins in membrane vesicle assembly. Science **349,** 195-198.

Donohoe BS, Kang BH, Staehelin LA. 2007. Identification and characterization of COPIa- and COPIb-type vesicle classes associated with plant and algal Golgi. Proceedings of the National Academy of Sciences USA **104,** 163-168.

Du W, Tamura K, Stefano G, Brandizzi F. 2013. The integrity of the plant Golgi apparatus depends on cell growth-controlled activity of GNL1. Molecular Plant **6,** 905-915.

Du Z, Zhou X, Ling Y, Zhang Z, Su Z. 2010. agriGO: a GO analysis toolkit for the agricultural community. Nucleic Acids Research **38**, W64-W70.

Eugster A, Frigerio G, Dale M, Duden R. 2004. The alpha- and beta'-COP WD40 domains mediate cargo-selective interactions with distinct di-lysine motifs. Molecular Biology of the Cell **15,** 1011-1023.

Gao C, Cai Y, Wang Y, Kang BH, Aniento F, Robinson DG, Jiang L. 2014. Retention mechanisms for ER and Golgi membrane proteins. Trends in Plant Science **19,** 508-515.

Gao C, Christine K, Qu S, San MWY, Li KY, Lo SW, Jiang L. 2012. The Golgi-localized Arabidopsis Endomembrane Protein12 contains both endoplasmic reticulum export and Golgi retention signals at its C Terminus. Plant Cell **24**, 2086-2104.

Gaynor EC, Emr SD. 1997. COPI-independent anterograde transport: cargo-selective ER to Golgi protein transport in yeast COPI mutants. Journal of Cell Biology **136,** 789-802.

Gerich B, Orci L, Tschochner H, Lottspeich F, Ravazzola M, Amherdt M, Wieland F, Harter C. 1995. Non-clathrin-coat protein alpha is a conserved subunit of coatomer and in Saccharomyces cerevisiae is essential for growth. Proceedings of the National Academy of Sciences USA **92,** 3229-3233.

Guo Q, Vasile E, Krieger M. 1994. Disruptions in Golgi structure and membrane traffic in a conditional lethal mammalian cell mutant are corrected by epsilon-COP. Journal of Cell Biology **125,** 1213-1224.

Hara-Kuge S, Kuge O, Orci L, Amherdt M, Ravazzola M, Wieland FT, Rothman JE. 1994. *En bloc* incorporation of coatomer subunits during the assembly of COP-coated vesicles. Journal of Cell Biology **124**, 883-92.

Jackson LP. 2014. Structure and mechanism of COPI vesicle biogenesis. Current Opinion in Cell Biology **29,** 67-73.

Jackson LP, Lewis M, Kent HM, Edeling MA, Evans PR, Duden R, Owen DJ. 2012. Molecular basis for recognition of dilysine trafficking motifs by COPI. Developmental Cell **23,** 1255-1262.

Kleinboelting N, Huep G, Kloetgen A, Viehoever P, Weisshaar B. 2012. GABI-Kat SimpleSearch: new features of the *Arabidopsis thaliana* T-DNA mutant database. Nucleic Acids Research **40,** D1211-1215.

Langhans M, Marcote MJ, Pimpl P, Virgili-López G, Robinson DG, Aniento F. 2008. In vivo trafficking and localization of p24 proteins in plant cells. Traffic **9,** 770-785.

Montesinos JC, Sturm S, Langhans M, Hillmer S, Marcote MJ, Robinson DG, Aniento F. 2012. Coupled transport of Arabidopsis p24 proteins at the ER-Golgi interface. Journal of Experimental Botany **63,** 4243-4261.

Montesinos JC, Langhans M, Sturm S, Hillmer S, Aniento F, Robinson DG, Marcote MJ. 2013. Putative p24 complexes in Arabidopsis contain members of the delta and beta subfamilies and cycle in the early secretory pathway. Journal of Experimental Botany **64,** 3147-3167.

Montesinos JC, Pastor-Cantizano N, Robinson DG, Marcote MJ, Aniento F. 2014. Arabidopsis p24delta5 and p24delta9 facilitate Coat Protein I-dependent transport of the K/HDEL receptor ERD2 from the Golgi to the endoplasmic reticulum. Plant Journal **80,** 1014-1030.

Nagashima Y, Mishiba K, Suzuki E, Shimada Y, Iwata Y, Koizumi N. 2011. Arabidopsis IRE1 catalyses unconventional splicing of bZIP60 mRNA to produce the active transcription factor. Science Reports **1,** 29.

Nakano RT, Matsushima R, Ueda H, Tamura K, Shimada T, Li L, Hayashi Y, Kondo M, Nishimura M, Hara-Nishimura I. 2009. GNOM-LIKE1/ERMO1 and

SEC24a/ERMO2 are required for maintenance of endoplasmic reticulum morphology in Arabidopsis thaliana. Plant Cell **21,** 3672-3685.

Ortiz-Masia D, Perez-Amador MA, Carbonell J, Marcote MJ. 2007. Diverse stress signals activate the C1 subgroup MAP kinases of Arabidopsis. FEBS Letters **581,** 1834-1840.

Osterrieder A, Hummel E, Carvalho CM, Hawes C. 2010. Golgi membrane dynamics after induction of a dominant-negative mutant Sar1 GTPase in tobacco. Journal of Experimental Botany **61**, 405–422.

Pastor-Cantizano N, Montesinos JC, Bernat-Silvestre C, Marcote MJ, Aniento F. 2016. p24 family proteins: key players in the regulation of trafficking along the secretory pathway. Protoplasma **253**, 967-985.

Pfaffl MW. 2004. Quantification strategies in real-time PCR**.** In: Bustin SA, ed. *A-Z of quantitative PCR.* La Jolla, CA, USA: International University Line (IUL), 87 – 112**.**

Richter S, Geldner N, Schrader J, Wolters H, Stierhof YD, Rios G, Koncz C, Robinson DG, Jurgens G. 2007. Functional diversification of closely related ARF-GEFs in protein secretion and recycling**.** Nature **448**, 488–492.

Robinson DG, Herranz MC, Bubeck J, Pepperkok R, Ritzenthaler C. 2007. Membrane dynamics in the early secretory pathway. Critical Reviews in Plant Sciences **26**, 199–225.

Sancho-Andrés G, Soriano-Ortega E, Gao C, Bernabé-Orts JM, Narasimhan M, Müller AO, Tejos R, Jiang L, Friml J, Aniento F, Marcote MJ. 2016. Sorting motifs involved in the trafficking and localization of the PIN1 auxin efflux carrier. Plant Physiology **171**, 1965-1982.

Song ZT, Sun L, Lu SJ, Tian Y, Ding Y, Liu JX. 2015. Transcription factor interaction with COMPASSlike complex regulates histone H3K4 trimethylation for specific gene expression in plants. Proc Natl Acad Sci U S A. **112**, 2900–2905.

Styers ML, O'Connor AK, Grabski R, Cormet-Boyaka E, Sztul E. 2008. Depletion of beta-COP reveals a role for COP-I in compartmentalization of secretory compartments and in biosynthetic transport of caveolin-1. American Journal of Physiology - Cell Physiology **294,** C1485-1498.

Teh OK, Moore I. 2007. An ARF-GEF acting at the Golgi and in selective endocytosis in polarized plant cells. Nature **448,** 493-496.

Tse YC, Mo B, Hillmer S, Zhao M, Lo SW, Robinson DG, Jiang L. 2004. Identification of multivesicular bodies as prevacuolar compartments in *Nicotiana tabacum* BY-2 cells. Plant Cell **16**, 672-693.

Vera-Sirera F, De Rybel B, Urbez C, Kouklas E, Pesquera M, Alvarez-Mahecha JC, Minguet EG, Tuominen H, Carbonell J, Borst JW, Weijers D, Blazquez MA. 2015. A bHLH-Based Feedback Loop Restricts Vascular Cell Proliferation in Plants. Developmental Cell **35,** 432-443.

Woo CH, Gao C, Yu P, Tu L, Meng Z, Banfield DK, Yao X, Jiang L. 2015. Conserved function of the lysine-based KXD/E motif in Golgi retention for endomembrane proteins among different organisms. Molecular Biology of the Cell **26,** 4280-4293.

Zanetti G, Pahuja KB, Studer S, Shim S, Schekman R. 2011. COPII and the regulation of protein sorting in mammals. Nature Cell Biology **14,** 20-28.

Zimmermann P, Hirsch-Hoffmann M, Hennig L, Gruissem W. 2004. GENEVESTIGATOR. Arabidopsis microarray database and analysis toolbox. Plant Physiology **136,** 2621-2632.

FIGURE LEGENDS

Figure 1. Characterization of *α1-cop-1* mutant.

A. Diagram of the *α1-COP* gene and localisation of the T-DNA insertion (triangle) in the *α1-cop-1* mutant. Black boxes represent coding regions and grey boxes represent 5'-UTR and 3'-UTR regions.The positions of RPα1, LPα1, α125 and α123 primers are shown.

B. sqRT-PCR analysis to show the absence of *α1-COP* mRNA in the *α1-cop-1* mutant. Total RNA from 7-day-old seedlings of the mutant and wild type (Col-0) were used for the RT-PCR. In the PCR, RPα1/LPα1 *α1-COP* gene specific primers and 36 cycles were used. *ACT7* was used as a control (22 cycles).

C. *α1-cop-1* mutant did not show a phenotype different from that of wild type.

Figure 2. Characterization of *α2-cop* mutants.

A. Diagram of the *α2-COP* gene and localisation of the T-DNA insertion (triangles) in the *α2-cop* mutants. Black boxes represent coding regions and grey boxes represent 5'-UTR and 3'-UTR regions.The positions of RPGα2, LPGα2, α125 and α123 primers are shown.

B. sqRT-PCR analysis to show the absence of *α2-COP* mRNA in the *α2-cop* mutants. Total RNA from 7-day-old seedlings of the mutants and wild-type (Col-0) were used for the RT-PCR. In the PCRs, gene specific primers and 36 cycles were used (Table S6). *ACT7* was used as a control (22 cycles).

C. Phenotype of 4-week-old (left) and 7-day-old (right) seedlings of wild type and *α2-cop-3* mutant.

D. Rescue of the growth phenotype of *α2-cop-3* by transformation with a HA tagged *α2-COP* cDNA construct. Phenotypes of 7-day-old seedlings (left) and 50-day-old plants (middle) of wild-type (Col-0), *α2-cop-3* and *α2-cop-3* complemented with α2-COP-HA. Western blot analysis with a HA antibody of the two independent lines of *α2-cop-3* transformed with α2-COP-HA shown in the middle.

Figure 3. Expression levels of *α-COP* in *α1-cop-1* and *α2-cop-3* mutants.

sqRT-PCR analysis of *α-COP* with α125 and α123 primers. Total RNA was isolated from 7-day-old seedlings of wild type (Col-0), *α1-cop-1* and *α2-cop-3* mutants. *ACT7* was used as a control (22 cycles).

A. Total *α-COP* expression in wild type and *α1-cop-1* mutant.

B. Total *α-COP* expression in wild type and *α2-cop-3* mutant.

C. Quantification of the experiments shown in A and B from three biological samples. Values were normalized against the *α-COP* fragment band intensity in wild type that was considered as 100%. Error bars represent SE of the mean.

D. Western blot analysis of total protein extracts from 7-day-old seedlings of wild type, *α1-cop-1* and *α2-cop-3* mutants with an N-terminal α-COP peptide antibody to detect both isoforms. 10 μg of total protein was load in every lane. GAPC was used as loading control.

Figure 4. *α2-cop-3* mutant shows abnormal distribution of RFP- p24δ5.

CLSM of epidermal cells of 4.5-DAG cotyledons. RFP-p24δ5 mainly localized to the ER network in wild-type plants (Col-0). In contrast, it was mostly found in punctate structures, which often appeared in clusters, in the *α2-cop* mutant. Scale bars: 10 μm**.**

Figure 5. *α2-cop-3* mutant shows abnormal distribution of the Golgi marker ST-YFP.

CLSM of epidermal cells of 4.5-DAG cotyledons. The Golgi marker ST-YFP partially localised to the ER network and to clusters of punctate structures in the *a2-cop-3* mutant**.** Scale bar is 10 μm**.**

Figure 6. Alteration of Golgi morphology of cotyledon cells in the *α2-cop-3* mutant**.**

A. Chemically fixed cotyledon cells from 4 days old wild-type (Col-0) or *α2-cop* mutant seedlings. Scale bars: 200 nm.

B. High-pressure frozen cotyledon cells from from 4 days old *α2-cop* mutant seedlings. G, Golgi; V, vesicle; MVB, multivesicular body. Scale bars: 500 nm.

Figure 7. Expression of specific genes in *α1-cop-1*, *α2-cop-3* and *gnll1* mutants.

A. sqRT-PCR validation of the microarray data performed for four genes whose expression changed in the *α2-cop-3* mutant. Total RNA was extracted from 4 day-old seedlings. Specific primers were used and *ACT7* was used as a control.

B. RT-qPCR analysis of SEC31A and SEC31B expression in *α1-cop-1* and *α2-cop-3* mutants. Total RNA was extracted from 7-day-old seedlings. The mRNA was analysed by RT-qPCR with specific primers and normalized to UBQ10 gene expression. Results are from two biological samples and three technical replicates. mRNA levels are expressed as relative expression levels and represent fold changes of mutant/wild type. Values represent mean ± SE of the two biological samples.

C. sqRT-PCR analysis of COPII subunit genes in the *α2-cop-3* mutant. Total RNA was extracted from 4-day-old seedlings. Specific primers were used and *ACT7* was used as a control.

D. sqRT-PCR analysis of *SEC31A*, *BIP3* and *PILS4* (genes that show altered expression in *α2-cop-3*) in *gnl1* (SALK_091078C). Total RNA was extracted from 4-day-old seedlings. Specific primers were used and *ACT7* was used as a control. The pattern of expression of the three genes is similar in both *α2-cop-3* and *gnl1*.

All specific primers are shown in Supplemental Table S6.

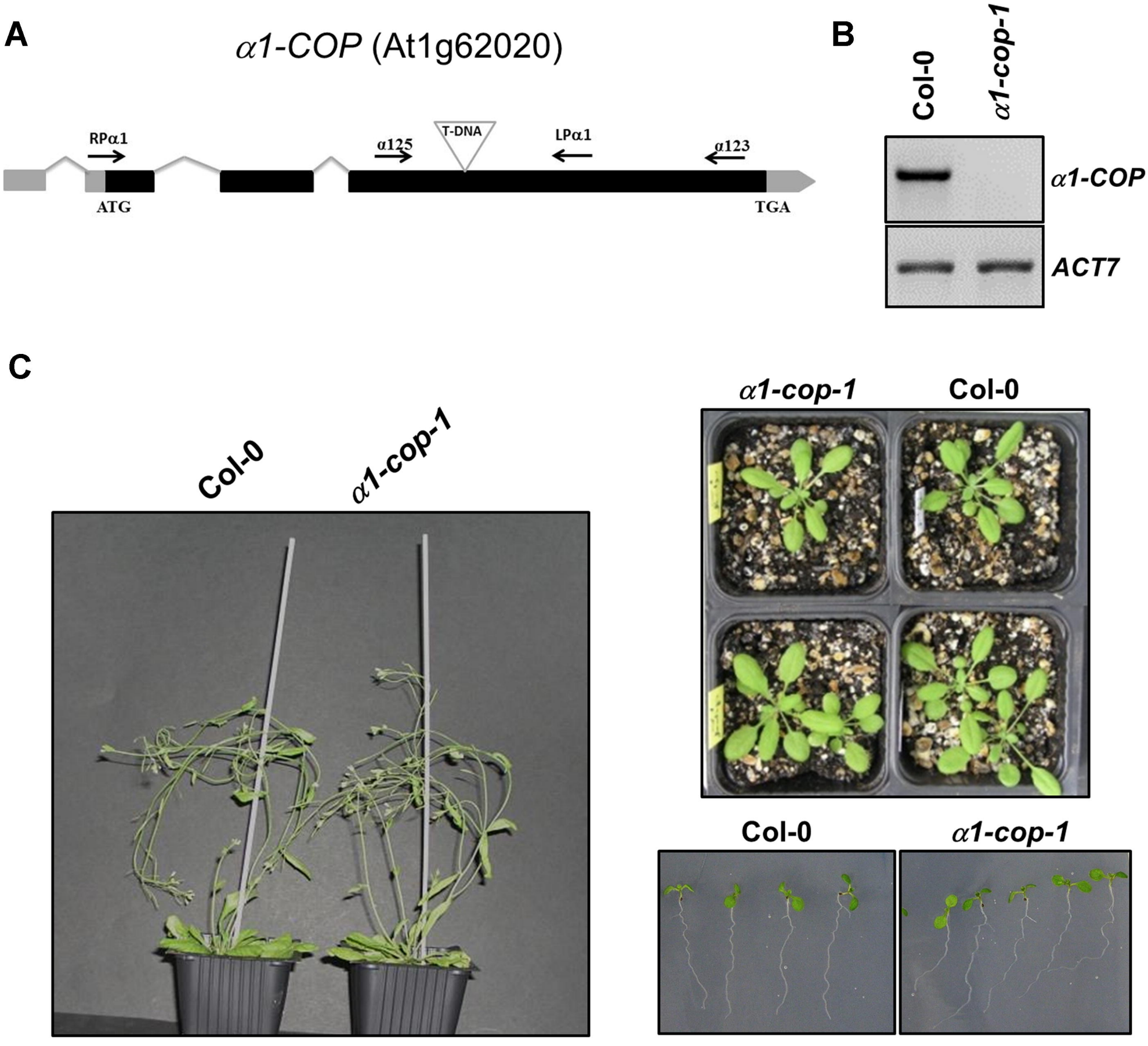
A
α1-COP (At1g62020)
RPα1
α125
T-DNA
LPα1
α123
ATG
TGA
B
Col-0
α1-cop-1
α1-COP
ACT7
C
Col-0
α1-cop-1
α1-cop-1
Col-0
Col-0
α1-cop-1

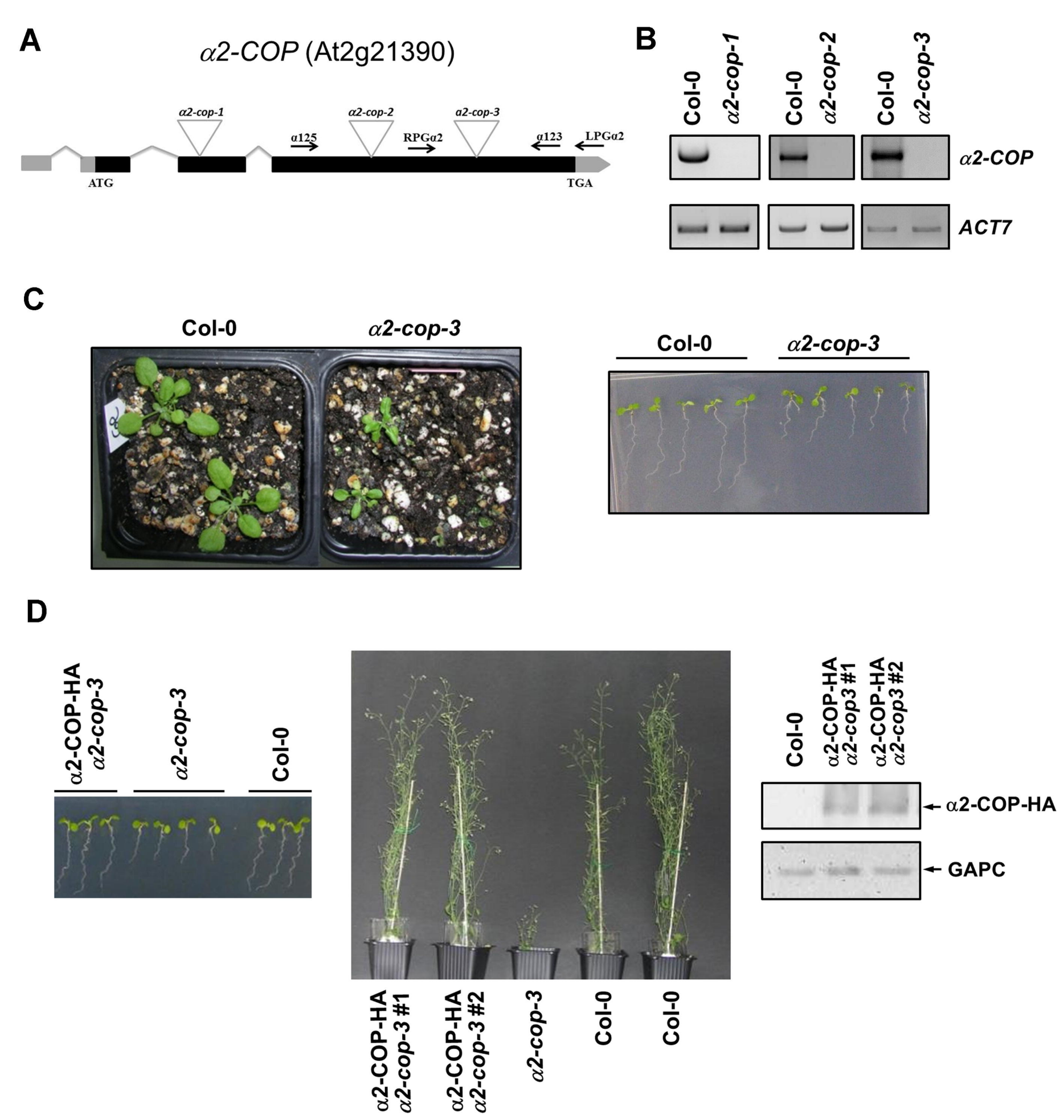
A
α2-COP (At2g21390)
α2-cop-1
α2-cop-2
α2-cop-3
α125
RPGα2
α123
LPGα2
ATG
TGA
B
Col-0
α2-cop-1
Col-0
α2-cop-2
Col-0
α2-cop-3
α2-COP
ACT7
C
Col-0
α2-cop-3
Col-0
α2-cop-3
D
α2-COP-HA α2-cop-3
α2-cop-3
Col-0
α2-COP-HA α2-cop-3 #1
α2-COP-HA α2-cop-3 #2
α2-cop-3
Col-0
Col-0
Col-0
α2-COP-HA α2-cop3 #1
α2-COP-HA α2-cop3 #2
α2-COP-HA
GAPC

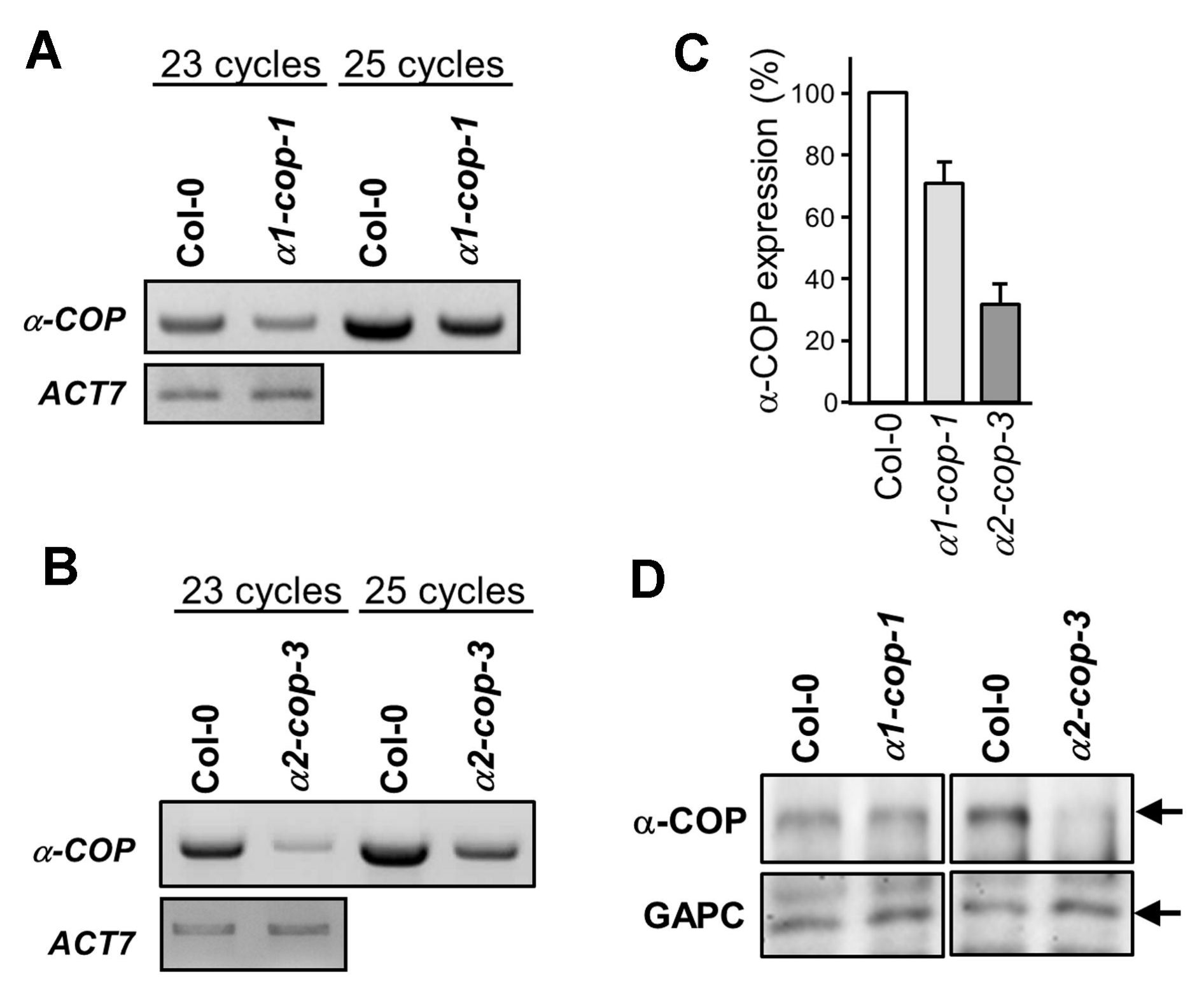
A
23 cycles
25 cycles
Col-0
α1-cop-1
Col-0
α1-cop-1
α-COP
ACT7
B
23 cycles
25 cycles
Col-0
α2-cop-3
Col-0
α2-cop-3
α-COP
ACT7
C
α-COP expression (%)
100
80
60
40
20
0
Col-0
α1-cop-1
α2-cop-3
D
Col-0
α1-cop-1
Col-0
α2-cop-3
α-COP
GAPC

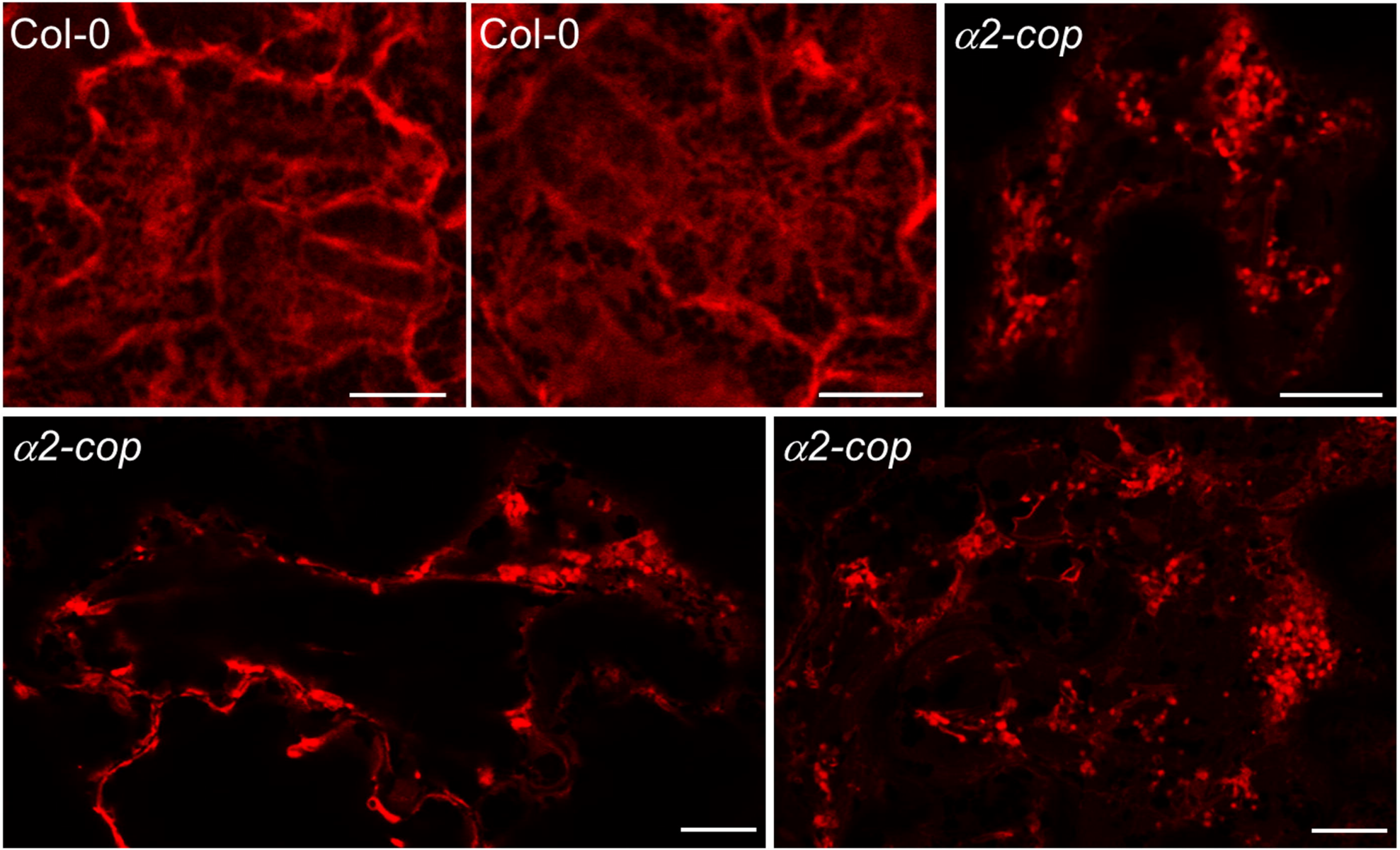
Col-0
Col-0
α2-cop
α2-cop
α2-cop

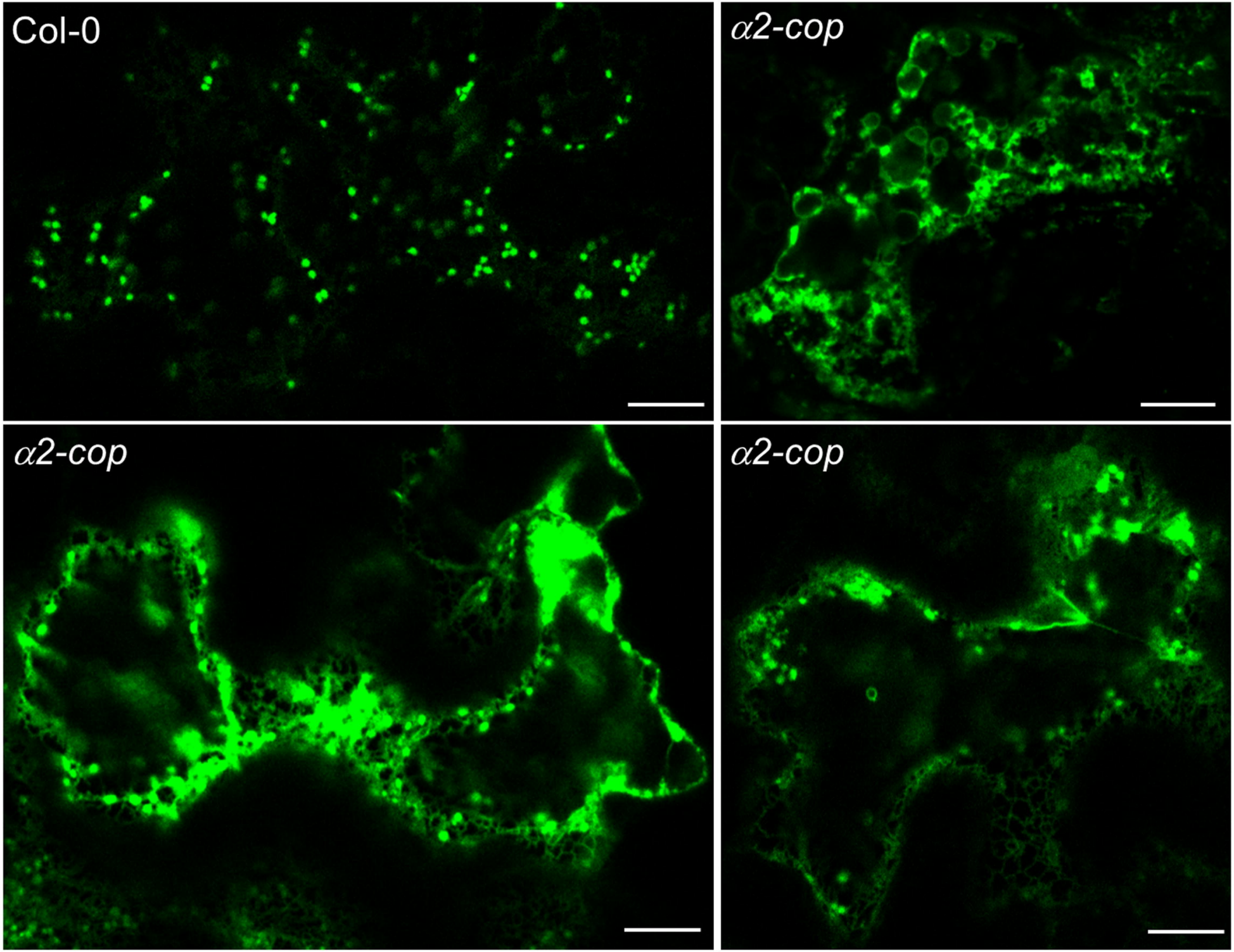
Col-0
α2-cop
α2-cop
α2-cop

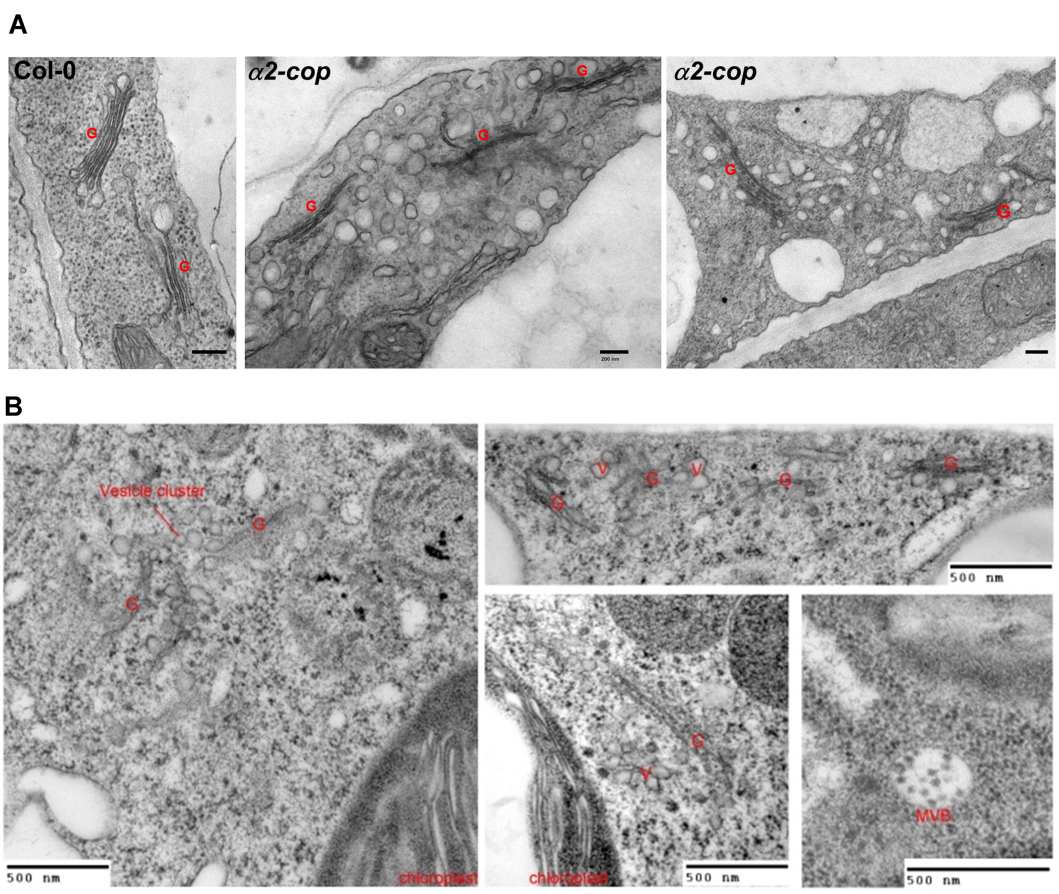
A
Col-0
α2-cop
α2-cop
G
B
Vesicle cluster
C
V
500 nm
chloroplast
MVB

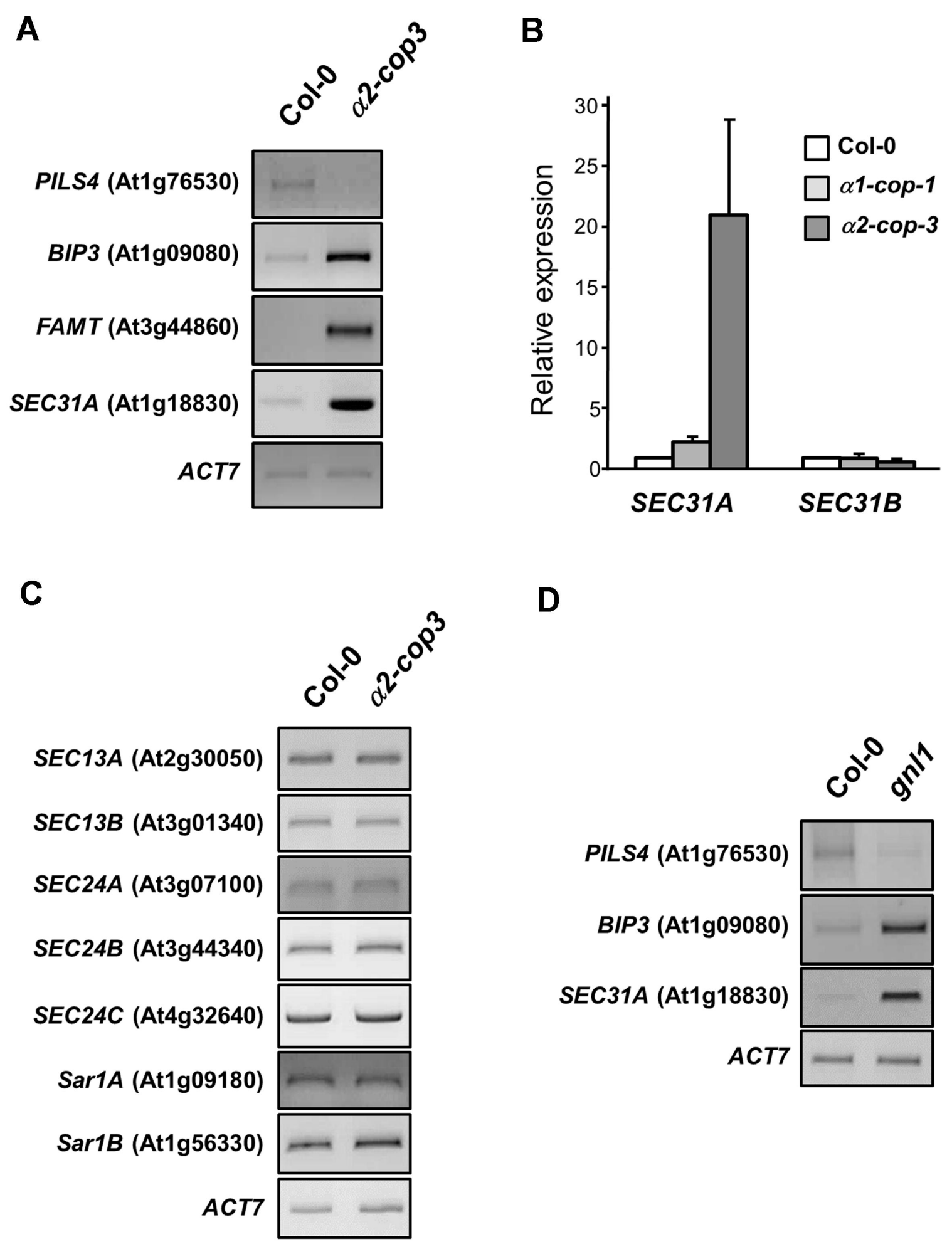
A
Col-0
α2-cop3
PILS4 (At1g76530)
BIP3 (At1g09080)
FAMT (At3g44860)
SEC31A (At1g18830)
ACT7
B
Relative expression
30
25
20
15
10
5
0
Col-0
α1-cop-1
α2-cop-3
SEC31A
SEC31B
C
Col-0
α2-cop3
SEC13A (At2g30050)
SEC13B (At3g01340)
SEC24A (At3g07100)
SEC24B (At3g44340)
SEC24C (At4g32640)
Sar1A (At1g09180)
Sar1B (At1g56330)
ACT7
D
Col-0
gnl1
PILS4 (At1g76530)
BIP3 (At1g09080)
SEC31A (At1g18830)
ACT7